Neuron, Vol. 40, 631–642, October 30, 2003, Copyright ©2003 by Cell Press

A Higher Order Motion Region in Human Inferior Parietal Lobule: Evidence from fMRI

Kristl G. Claeys,[1,2] Delwin T. Lindsey,[3] Erik De Schutter,[2] and Guy A. Orban[1,*]
[1]Laboratorium voor Neuro- en Psychofysiologie
Katholieke Universiteit Leuven
Campus Gasthuisberg
Herestraat 49
Leuven B-3000
Belgium
[2]Laboratorium voor Theoretische Neurobiologie
Universitaire Instelling Antwerpen
Universiteitsplein 1
Wilrijk B-2610
Belgium
[3]Department of Psychology
The Ohio State University
Mansfield, Ohio 44906

Summary

The proposal that motion is processed by multiple mechanisms in the human brain has received little anatomical support so far. Here, we compared higher- and lower-level motion processing in the human brain using functional magnetic resonance imaging. We observed activation of an inferior parietal lobule (IPL) motion region by isoluminant red-green gratings when saliency of one color was increased and by long-range apparent motion at 7 Hz but not 2 Hz. This higher order motion region represents the entire visual field, while traditional motion regions predominantly process contralateral motion. Our results suggest that there are two motion-processing systems in the human brain: a contralateral lower-level luminance-based system, extending from hMT/V5+ into dorsal IPS and STS, and a bilateral higher-level saliency-based system in IPL.

Introduction

Ever since the studies by Exner (1875) and early 20th century Gestalt psychologists (e.g., Wertheimer, 1912), a great deal of effort has been directed towards understanding how humans perceive motion. In the last 30 years, the dominant theoretical position has been that motion perception does not have a single underlying substrate, but results from the action of multiple, distinct mechanisms. Braddick (1974) distinguished between short- and long-range mechanisms based on spatio-temporal factors. Chubb and Sperling (1988) emphasized luminance-based first-order versus non-Fourier second-order motion processing. It is not clear, though, whether these distinctions characterize critical differences in the computational mechanisms or neural substrates of human motion processing (Cavanagh and Mather, 1989; Smith et al., 1998; Vaina et al., 1999; Dupont et al., 2003; Seiffert et al., 2003).

*Correspondence: guy.orban@med.kuleuven.ac.be

More recently, psychophysical experiments using equiluminant color stimuli have suggested another distinction. Both Cavanagh (1992) and Sperling and coworkers (Lu and Sperling, 1995; Lu et al., 1999a, 1999b) distinguish between low-level, luminance-based preattentive processes, and high-level processes engaged by attention to salient moving features. Previous functional magnetic resonance imaging (fMRI) studies have revealed a number of motion-processing regions, including the human middle temporal complex (hMT/V5+), human visual area V3A, superior temporal sulcus (STS), and several intraparietal sulcus (IPS) regions (Zeki et al., 1991; Tootell et al., 1995, 1997; Puce et al., 1998; Sunaert et al., 1999). These regions respond to simple moving gratings and random dot patterns, and their reaction is preattentive (Rees et al., 1997; Vanduffel et al., 2002), even though attention can modulate their activity (Culham et al., 1998, 2001). Hence, they are a likely substrate of the lower-level motion system. To date, no neural substrate of a higher-level attention-based motion system has been documented. The goal of the present study was (1) to identify the neural substrate of the higher-level motion system and (2) to contrast it to the traditional motion areas.

To address these issues we recorded fMRI responses to four kinds of stimuli designed to preferentially engage higher- or lower-level motion systems (Table 1). The first consisted of isoluminant sinewave gratings, produced by antiphase superposition of reddish and greenish component gratings of low-, medium-, and high-green saturation relative to the red components (Figure 1). According to Sperling and coworkers (Lu et al., 1999b), a high-level saliency-based motion mechanism will be engaged at isoluminance when grating components differ significantly in saturation, because the higher saturation component will become more salient perceptually. When grating saturations are similar, relative salience differences are diminished, neither grating component preferentially engages attention, and motion is not perceived. In the present experiments, relative saliency of the components was varied by manipulating the saturation of the green component while keeping the saturation of the red component fixed. The medium-green saturation condition corresponded to an approximate minimum in saliency, which we hereafter refer to as the "iso-saliency" condition. We hypothesized that brain regions that reflect motion processing based on saliency will show greater activation in low- and high-green saturation conditions than in the medium-green saturation condition. Isoluminance points for our gratings were determined in situ by motion nulling, a psychophysical technique described by Lu et al. (1999a, 1999b), for the photometric matching of two lights of different wavelength composition. Isoluminance points for our grating stimuli were determined immediately before each of the six scanning sessions per subject. We also employed a luminance-modulated, achromatic sinewave grating as a lower order motion stimulus. The stimuli were positioned in the right visual field and moved up and down or remained stationary in separate scanning epochs.

Table 1. Subjects Participating in the Two Main and Six Control Experiments

Exp.	Main I	Control 1	Control 2	Main II	Control 3	Control 4	Control 5	Control 6
Order	higher (Sa)	higher (Sa)	first	higher (AM)	higher (AM)	higher (AM)	second (CH)	second (DN)
Task	no	no	no	no	no	↑ temp. freq. det.[a]	no	no
VF	R	L	R, L, C	R, L	R, L, C	R, L	C	C
Sess./subj.	6	2	1	1	1	1	1	1
S1	*	*	*	*				
S2	*	*	*	*			*	*
S3	*	*	*	*				
S4	*		*					
S5	*		*					
S6	*		*					
S7			*	*		*	*	*
S8			*	*		*	*	*
S9			*	*	*	*	*	
S10			*	*	*	*	*	
S11			*	*		*	*	
S12			*	*		*	*	
S13				*				
S14				*				
S15				*				
Total	6	3	12	12	2	6	7	3

Sa, saliency-based motion; AM, apparent motion; CH, coherence; DN, density; VF, visual field; R, right; L, left; C, central.
[a] Detection of increasing temporal frequency.

When subjects had completed all six scanning sessions, each was asked to rate their levels of attention to the stimuli across the different sessions.

In a second series of recordings we used moving luminance-modulated random dot textures positioned in the central, left, and right visual field. A number of previous studies (Zeki et al., 1991; Tootell et al., 1995; Sunaert et al., 1999) have shown that these first-order stimuli are potent activators of classical motion centers. The third series of recordings employed an oscillating apparent motion quartet. The stimuli we employed are thought to tap the hypothesized higher-level motion system (Battelli et al., 2001). The fourth and final set of experiments were performed using contrast modulated checkerboard stimuli described by Vaina and Cowey (1996). These stimuli were used to tap second-order motion processing and to clarify the relationship between second-order motion processing and the hypothetical higher-level motion system.

Analysis of brain responses within and across these four classes of stimuli—isoluminant and luminance-modulated gratings, random dot textures, the apparent motion quartet, and contrast modulated checkerboards—provides compelling evidence for separate neural substrates for lower- and higher-level motion systems. The latter system appears to be localized in the inferior parietal lobule (IPL).

Results

Subjects maintained fixation very well during scanning. The average frequency of saccades was less than 0.7 per condition for all time series in all fMRI studies. The frequency of eye movements did not differ significantly among conditions for any session of any experiment (Friedman ANOVA; main exp. 1: $p > 0.12$; control exp. 2: $p > 0.20$; main exp. 2: $p > 0.11$; control exp. 4: $p > 0.84$; control exp. 5: $p > 0.25$).

In the analysis of main experiment 1, we first tested for higher-level motion regions by contrasting the motion and stationary control conditions of the salience-defined stimuli, averaged over the high- and low-green saturation conditions (Figure 2). We observed significant ($p < 0.05$ corrected for multiple comparisons) activation in the right inferior parietal lobule (IPL), ipsilaterally to the stimulation, and bilaterally in area hMT/V5+ (Figure 2A). The functional profiles of the IPL region revealed

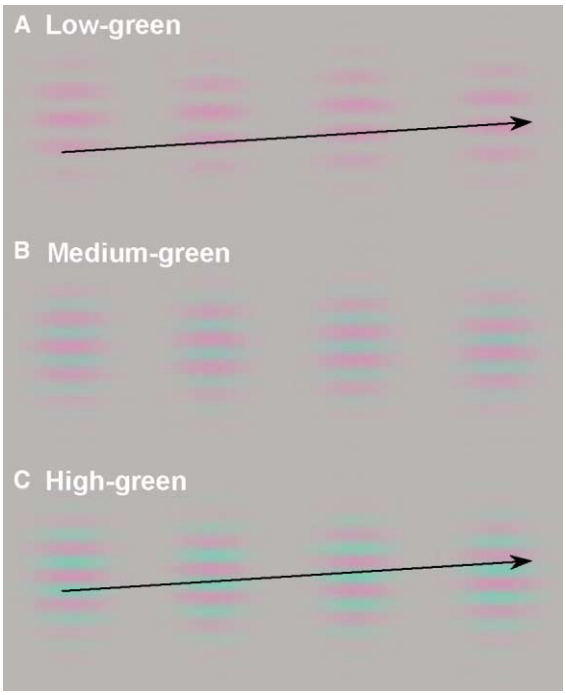

Figure 1. Stimulus Configuration in Main Experiment 1 and Control 1
Stimuli in the low-green (A), medium-green (B), and high-green (C) saturation isoluminant conditions are shown. The black arrow indicates the direction of the perceived motion.

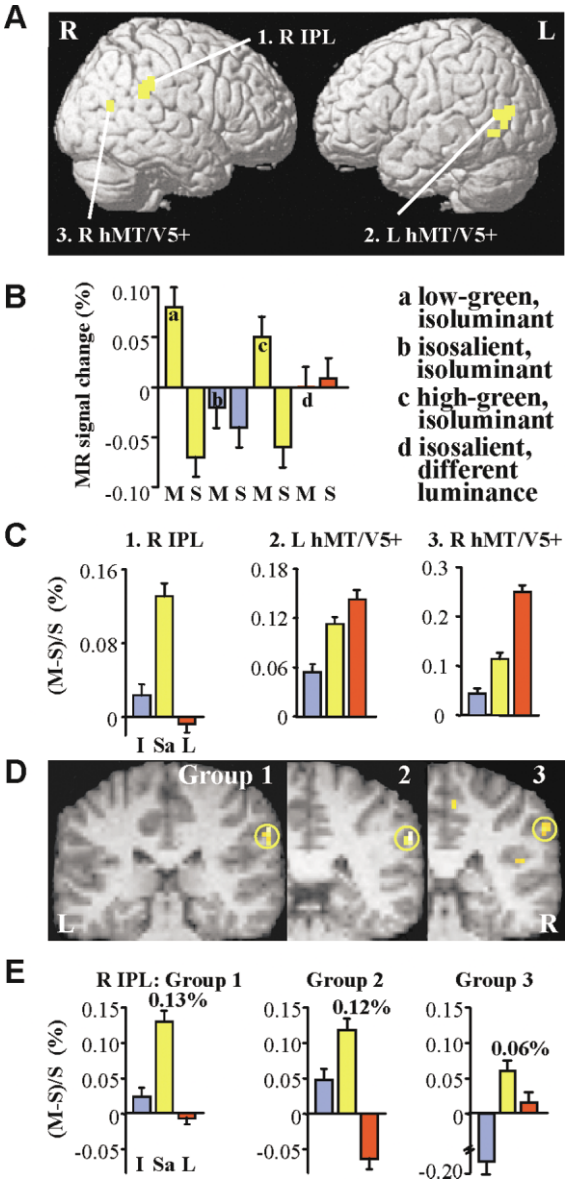

Figure 2. The Higher-Level Feature-Tracking Motion System: Main Experiment 1

(A) Statistical parametric maps (SPMs) showing voxels significant ($p < 0.05$ corrected for multiple comparisons) in the group analysis (main experiment 1, two highest attention scan sessions) for the subtraction moving minus stationary in the different salience conditions, rendered on the standard right and left hemispheres.

(B) Activity profile of R IPL (66, −36, 33) in which the relative (to fixation) adjusted MR signal is plotted as a function of the eight stimulus conditions: moving (M) and stationary (S) stimuli in the isosalient (b)-isoluminant (blue), different salience (a and c) -isoluminant (yellow), and isosalient-different luminance (d, red) conditions; letters as in Figure 1.

(C) Functional profiles of R IPL, L hMT/V5+ (−42, −66, 12), and R hMT/V5+ (54, −66, 15) plotting the average percentage MR signal change (M-S/S) for the moving (M) compared to the stationary (S) stimuli in the isosalient-isoluminant (I, blue), different salience-isoluminant (Sa, yellow), and isosalient-different luminance (L, red) conditions.

(D) SPMs of the three group analyses for the subtraction as in (A), projected onto a coronal slice selected to show the R IPL activation: group 1 (highest attention sessions): 66, −36, 33; group 2: 66, −30, 39; group 3 (lowest attention sessions): 66, −33, 39; 1 and 2 at $p < 0.05$ corr., 3 at $p < 0.001$ uncorr.

activity only for salience-defined motion, which was similar in the low- and high-green saturation conditions (Figure 2B). This is summarized in a profile plotting the motion response for the three conditions (Figure 2C): isosalience-isoluminant (blue), different saliency (yellow), and different luminance (red). On the other hand, hMT/V5+ showed MR activity for motion driven by red/green salience differences but even more so for motion driven by achromatic luminance differences. That right (R) IPL was not driven by luminance-based motion was confirmed by exclusive masking (in the analysis) of the response to salience-based motion by the response to luminance-based motion ($z = 5.86$, $p < 0.05$ corr.). The right IPL region fits our expectation for a higher-level motion region, but in addition, fails to respond to lower-level, luminance-based motion.

To ensure the generality of the results, data obtained in the first experiment were subjected to three separate group analyses, each comprising two sessions, ranked according to the subject's own estimated level of attention to the stimuli and clarity of the attention-based motion percept. The results described so far (Figures 2A–2C) were obtained in a group analysis of the two highest attention scan sessions per subject. The results of the other two group analyses confirmed those of the first analysis (Figure 2D), although significance and magnitude of the IPL activation by salience-based motion was reduced in the analysis of the two lowest attention sessions (Figure 2E). These data also indicate that the salience-based motion was strong enough to obtain reliable activation of IPL in only two scanning sessions. Single-subject analyses confirmed the results of the group analysis. A right IPL activation was observed in each of the six subjects in the salience-defined motion conditions but not in the luminance-defined motion condition (Figures 3A and 3B). Furthermore, the right IPL activation by salience-based motion was significant ($z = 5.32$, $p < 0.05$ corr.) in a conjunction analysis across the six subjects (Friston et al., 1999) of the two highest attention sessions, underscoring again the generality of the results.

The activation of R IPL by a right-sided motion stimulus is consistent with either an ipsilateral or a bilateral representation of higher-level motion. In fact, in the group analysis of Figure 2A, the left (L) IPL (−63, −36, 39) reached a lower threshold ($z = 4.39$, $p < 0.001$ uncorrected for multiple comparisons) for salience-based motion, suggesting that the representation might be bilateral. To confirm this alternative, we enrolled three subjects (S1–S3) in a control experiment (Table 1) in which the stimuli were positioned in the left visual field (Figure 4). This control experiment revealed an activation ($p < 0.05$ corr.) of the L IPL region by salience-based motion only (Figure 4B), with the contralateral (right) IPL activated at a less significant ($p < 0.001$ uncorr.) level. The activity profiles confirm that the IPL region in both hemispheres represents salience-specific motion in the

(E) Functional profiles of right IPL in the three groups of two scanning sessions, each in decreasing order of attention to the stimulus motion. Percentages indicate size of saliency-based motion effect, other conventions as in (C). R, right; L, left; IPL, inferior parietal lobule; hMT/V5+, human middle temporal complex. Error bars indicate SD.

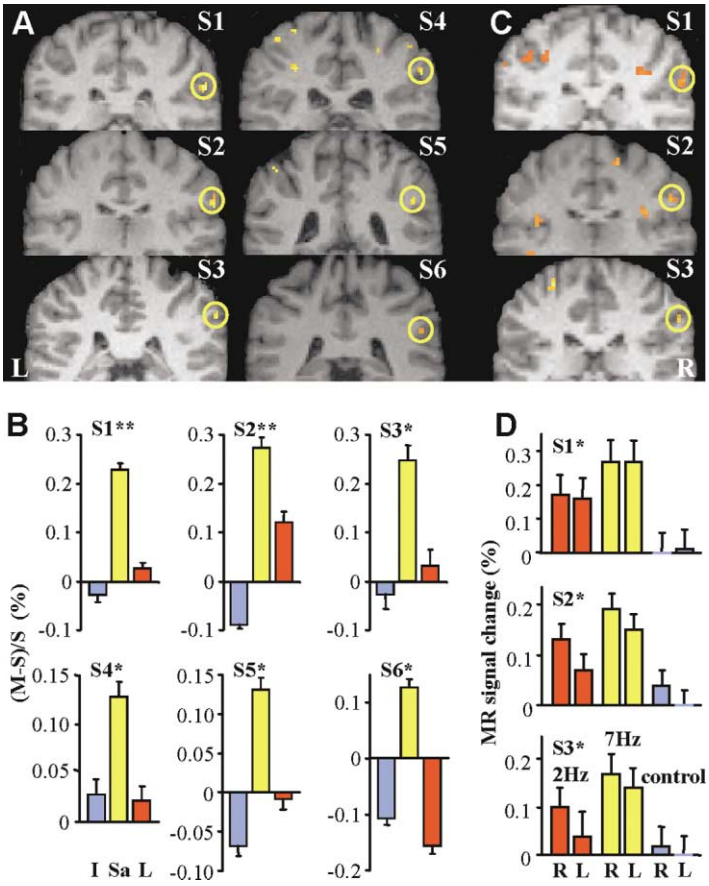

Figure 3. Right IPL Activation in Single Subjects

(A and C) SPMs showing the right IPL activation (encircled in yellow), in the single-subject analyses for the subtraction moving minus stationary different salience conditions in the first main experiment (A), and for the subtraction 7 Hz apparent motion minus 7 Hz control condition in the second main experiment (C), projected onto individual coronal sections selected to show R IPL. Significance reached $^{**}p < 0.05$ corrected and $^{*}p < 0.001$ uncorrected for multiple comparisons, as indicated per subject in (B and D). The IPL activation site is located superior to and nearby the lateral sulcus. Subjects 1–3 participated in both experiments. The location of their right IPL activation in the two experiments matches very well. The individual right IPL coordinates were S1: 64, −32, 28; S2: 68, −28, 30; S3: 68, −36, 38; S4: 62, −32, 38; S5: 52, −44, 32; S6: 56, −40, 28 for main experiment 1 and S1: 66, −33, 24; S2: 60, −24, 33; S3: 60, −27, 39 for main experiment 2.

(B and D) Corresponding activity profiles for the first ([B], same conventions as in Figure 1) and for the second (D) main experiment plotting % MR signal change for the 2 Hz (red) and 7 Hz (yellow) apparent motion conditions and the 7 Hz *control* condition (blue), for a stimulus located in the right (R) and left (L) visual field. For other conventions see legend Figure 2.

two hemifields, though ipsilateral responsiveness was stronger.

We next compared the motion regions activated in our first main experiment with the potential lower-level motion regions revealed in a second control experiment (same six participants, Table 1). The stimulus consisted of a moving or stationary random texture pattern, positioned in the central, left, and right visual field. We focus here on the results obtained for the right visual field in analogy with the main experiment. By contrasting the moving and stationary condition (Figure 5A), a predominantly left-sided, contralateral, activation pattern was observed, including area hV3A, hMT/V5+, superior temporal sulcus (STS), posterior insular cortex (PIC), parieto-occipital intraparietal sulcus (POIPS), dorsal intraparietal sulcus medial (DIPSM), and dorsal intraparietal sulcus anterior (DIPSA). This pattern corresponds to the known motion regions (Sunaert et al., 1999). Activity in all these left-sided regions was larger for contralateral (right) than ipsilateral (left) visual field stimulation (Figure 5B).

We then tested which of these traditional motion regions, mapped out in the control experiment, were activated by the salience-defined and luminance-defined motion in the first main experiment. As expected, all known motion areas were activated by luminance based-motion (Figure 5C). Many extrastriate areas, such as hV3A and hMT/V5+, also showed activity for salience-based motion, but far extrastriate motion areas STS and DIPSA revealed activity exclusively for luminance-defined motion. Notice that these two regions and also DIPSM and PIC did not respond to motion in the isoluminant-isosalient condition, in which little motion is perceived.

Since experiment 1 demonstrated that human R IPL is a higher order motion region, we wondered whether the IPL region processes other types of stimuli for which a higher-level status had been proposed. A recent human lesion study (Battelli et al., 2001) suggested that a quartet variant of the two dots apparent motion display (Figure 6A) (Ternus, 1938), which has previously been considered a long-range motion stimulus (Braddick, 1974), might be processed by the IPL. Patients with a unilateral R IPL lesion were shown to suffer from a bilateral deficit for long-range apparent motion, without deficit on lower order motion tests. Patients failed to distinguish apparent motion from flicker at high frequencies (6–8 Hz), but not at frequencies below 5 Hz.

Therefore, in the second main experiment (Table 1), we presented the quartet display with apparent motion at 2 Hz (Goebel et al., 1998) and 7 Hz, and a control flicker at 7 Hz, and positioned these stimuli in right and left visual fields. A stringent random-effect analysis (Friston et al., 1999) was performed on the group data ($n = 12$). Averaging over left and right visual field presentations, apparent motion at 7 Hz compared to flicker activated a similar R IPL region as in our first study (Figure 6B). The activation of the left IPL was weaker, but the activity profiles of the two IPL regions are similar, with equally large activity for 7 Hz apparent motion in both

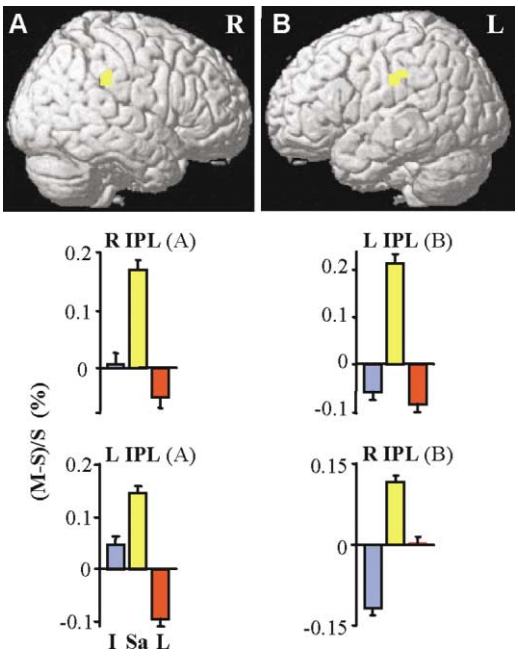

Figure 4. Bilateral Activation of IPL

SPMs as in Figure 2 but with an exclusive mask by the subtraction moving minus stationary different-luminance condition, for the stimulus positioned in right ([A], main experiment 1 but same three subjects as in control 1) and left ([B], first control experiment, n = 3) visual fields. This mask was used to reveal only brain regions that are specifically activated by salience-defined motion. In both experiments, ipsilateral IPL is significantly ($p < 0.05$ corr.) activated. Activation of contralateral IPL (data not shown) only reached $p < 0.001$ uncorr. Functional profiles of the right ([A]: 66, −33, 33; [B]: 66, −33, 39) and left ([A]: −57, −33, 39; [B]: −66, −27, 36) IPL are shown for the stimulus located in right (A) and left (B) visual fields. Conventions as in Figure 2.

visual hemifields (Figures 6C and 3D). Single-subject analysis, also averaged over left and right visual field presentations, confirmed the results of the group analysis: R IPL was activated ($p < 0.001$ uncorr.) in 10/12 subjects and L IPL in 8/12 subjects (Figure 6E). Responses in three of the subjects that participated in both main experiments are illustrated in Figures 3C and 3D to show that the location of the IPL activation in both main experiments was very similar. The only other significant ($p < 0.0001$ uncorr.) activation by 7 Hz apparent motion was bilateral hMT/V5+. No activation was observed in ventral visual regions, suggesting that the MR activation in temporal cortex by long-range apparent motion reported by Zhuo et al. (2003) reflects change in size rather than motion as such.

Testing the conditions of main experiment 2 on the lower-level motion regions revealed that these areas were generally responsive to the 2 Hz apparent motion, and in general responded predominantly to contralateral visual field stimulation (Figure 5D). Many of them were also responsive to apparent motion at 7 Hz. The two regions, however, which failed to respond to saliency-based motion in main experiment 1, DIPSA and STS, also failed to respond to the apparent motion at 7 Hz. Notice also that several regions especially the near extrastriate areas hV3A and hMT/V5+ responded to flicker. Flicker responses, however, were strongly reduced in those four regions that in main experiment 1 failed to respond in the isosaliency-isoluminance condition, STS, PIC, DIPSM, and DIPSA, confirming that these regions are active only in conditions in which motion is perceived.

The previous experiments indicate that IPL represents motion bilaterally in the visual field while the traditional motion regions represent predominantly motion in the contralateral field. To explore these differences more fully, we analyzed the response to the random texture motion presented in three positions (central and 5° peripheral in left and right visual field) in the second control experiment. Additionally, we measured in two subjects the response to apparent motion and flicker at 7 Hz in the same three positions (control experiment 3, Table 1). As shown in Figure 7, the traditional motion regions all had a clear bias in favor of the contralateral visual field and in most cases a higher magnification in the center of the visual field: their response to the central motion was stronger than to contralateral motion, even if the central stimulus was physically smaller. Weak responses to random texture motion, reaching only $p < 0.001$ uncorr. in the group analysis, were also observed in IPL, but here the response to ipsilateral motion was slightly stronger than to central or contralateral motion. With apparent motion, which was physically identical in all three stimulus positions, the ipsilateral response clearly exceeded the two other responses (Figure 7). Notice that the stronger response to ipsilateral stimulation than to contralateral stimulus is a constant feature of IPL since it was also observed in experiment 1 (Figure 4).

In order to control for possible differences in attention to the stimuli between the apparent motion and flicker control conditions of main experiment 2, we performed a control experiment (control 4, Table 1), in which six subjects detected an increase in the temporal frequency of the stimulus in either condition. Both right and left IPL (Figure 6D) were significantly ($p < 0.05$ corr.) more active in the apparent motion than the flicker condition. Thus, the activation of IPL by apparent motion does not reflect differences in attention to the stimulus.

Finally, we wanted to clarify the response of IPL to another type of nonluminance-based motion, second-order motion (Chubb and Sperling, 1988). We used the very same contrast-modulated checkerboard stimuli as Vaina and Cowey (1996) and Vaina et al. (1999) used to demonstrate a dissociation between first and second-order motion processing in patients. In control experiment 5 (Table 1) we manipulated the coherence of these stimuli just as Vaina et al. (1999) had done in their patients. In control experiment 6, we investigated the effect of density of the stimuli in a more restricted group of subjects (Table 1). This latter experiment demonstrated that in most visual cortical areas the middle density used in control experiment 5 and in Vaina et al.'s patients was near optimal. Using this middle density, the results of control experiment 5 revealed that in most lower-level motion regions, MR activity increased with motion coherence, as Rees et al. (2000) reported for first-order stimuli. A notable exception was hV3A, which responded strongly to low-coherence stimuli (Figure 5E). On the other hand, the higher-level motion IPL region responded little to these second-order motion stimuli, not

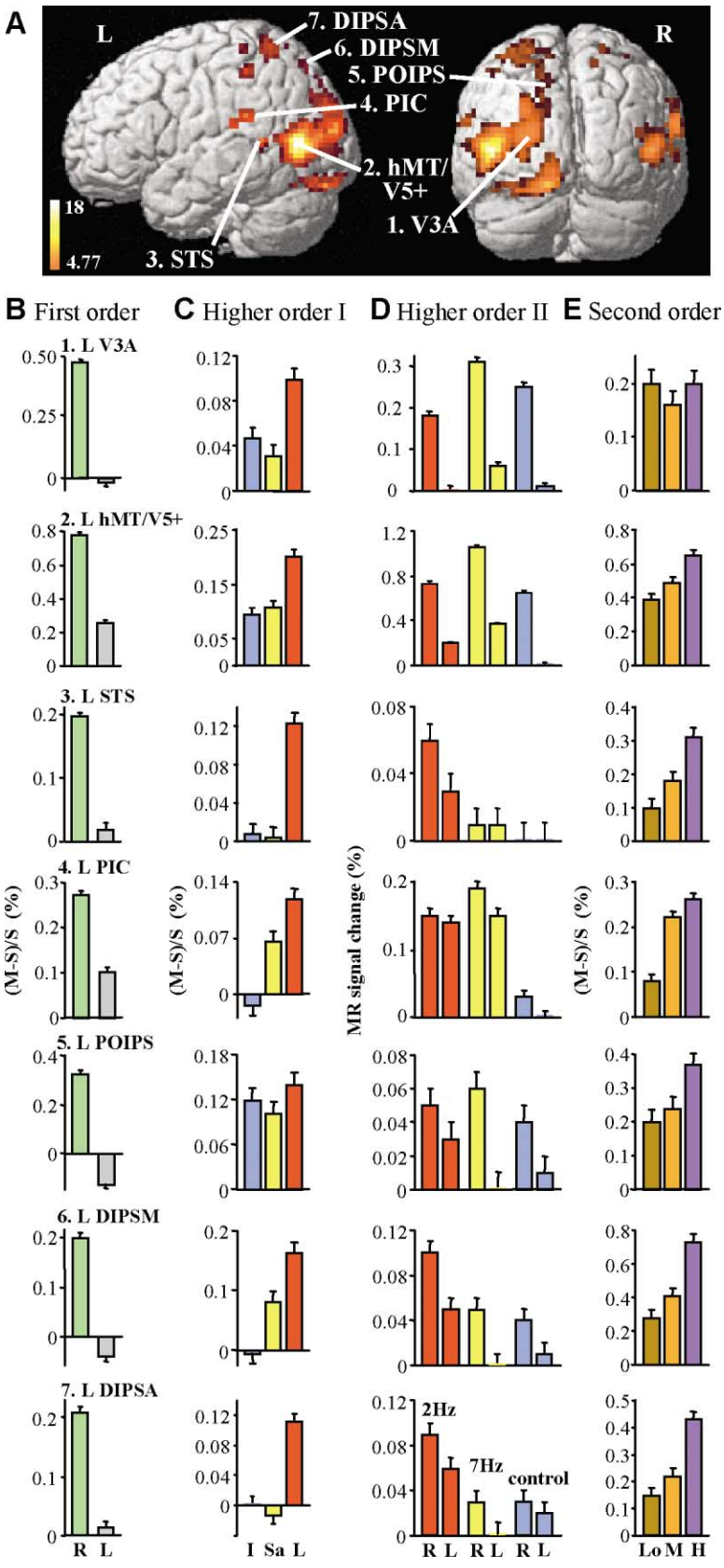

Figure 5. Cortical Regions of the Lower-Level Motion System

(A) Statistical parametric maps showing voxels significant ($p < 0.05$ corr.) in the group analysis for the subtraction moving minus stationary random texture stimulus (control experiment 2), superimposed on the left standard hemisphere in a lateral and posterior view. The stimulus was located in the right visual field. The color bar indicates z scores.

(B) Corresponding functional profiles of the main lower-level motion areas (see coordinates below) plotting % MR signal change (M-S/S) in the moving (M) compared to the stationary (S) conditions for a stimulus located in right (R), contralateral (green), and left (L), ipsilateral (gray) visual field.

(C and D) Activity profiles of these areas for the conditions of the first (C) and second (D) main experiment (local maxima in left hemisphere at $p < 0.001$ uncorr.).

(E) Activity profiles of these areas in control experiment 5 (average of R and L hemispheres, local maxima at $p < 0.001$ uncorr.) in the low (Lo, brown), medium (M, orange), and high (H, purple) coherence conditions. In (A) and (B) hV3A (−21, −90, 15), indicates human visual area 3A; hMT/V5+ (−42, −69, 6), human middle temporal complex; STS (−57, −48, 6), superior temporal sulcus; PIC (−51, −30, 21), posterior insular cortex; POIPS (−15, −84, 45), parieto-occipital intraparietal sulcus; DIPSM (−12, −63, 63), dorsal intraparietal sulcus medial; DIPSA (−30, −36, 63), dorsal intraparietal sulcus anterior. For other conventions see legend Figures 2 and 3.

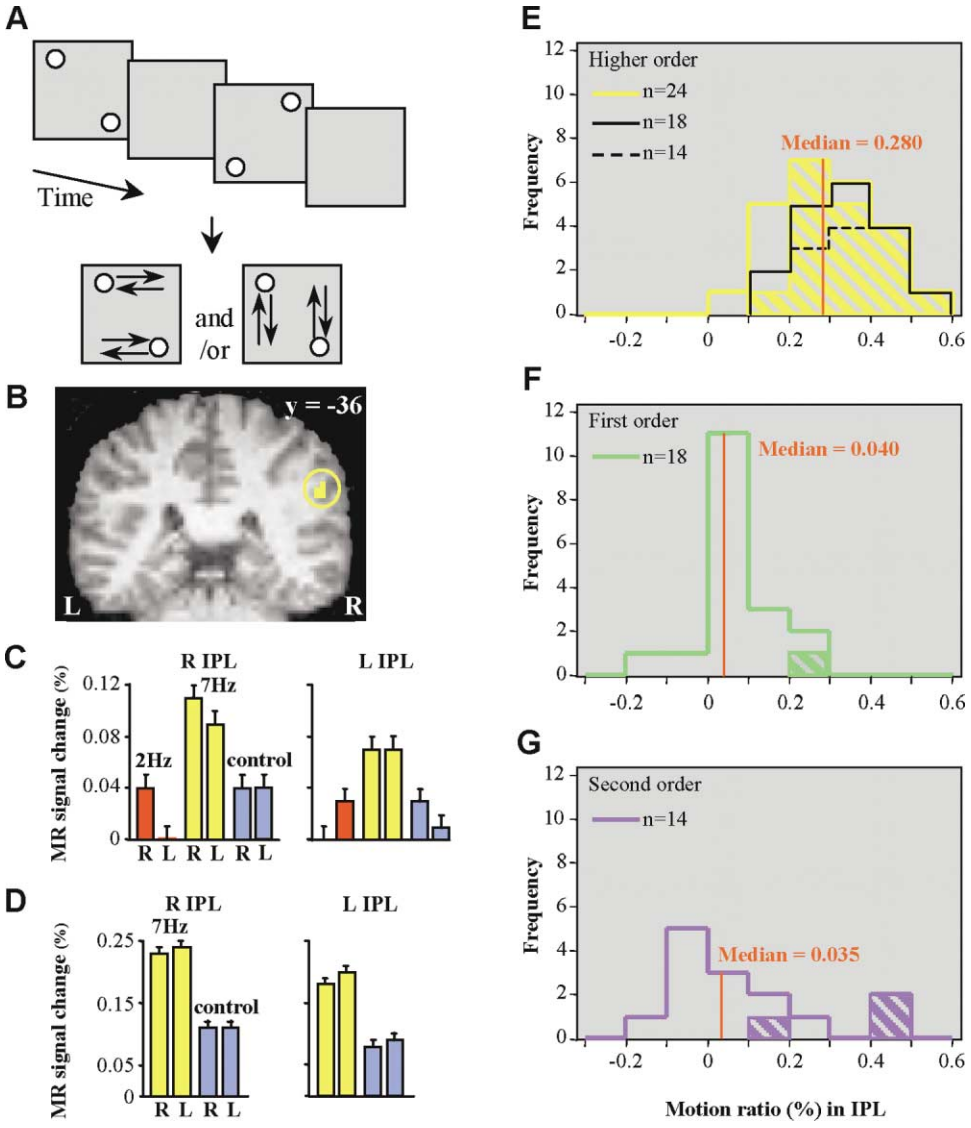

Figure 6. Response of IPL to Apparent Motion Stimulus

(A) Stimulus configuration in main experiment 2 and control 3 and 4.

(B) SPM showing the right IPL activation (60, −36, 30; encircled in yellow) in the random-effect group analysis (main experiment 2, colored voxels $p < 0.001$ uncorr.) for the subtraction 7 Hz apparent motion conditions minus 7 Hz control conditions, averaged over R and L presentations, overlaying an anatomical coronal slice at antero-posterior level y = −36 in Talairach space.

(C) Corresponding activity profiles of right IPL (see [B]) and left IPL (−57, −39, 36; random-effect group analysis, $p < 0.01$ uncorr.). Same conventions as in Figure 3.

(D) Activity profile of right (63, −36, 30; $p < 0.05$ corr.) and left IPL (−63, −39, 33; $p < 0.05$ corr.) in control experiment 4.

(E–G) Distributions of motion ratios (M-S/S) in individual hemispheres (n) of main experiment 2 (E), control experiment 2 (F) and control experiment 5 (G). Ratios were averaged over right and left stimulus presentations in (E) and (F) and over levels of coherence in (G). Hatched bars indicate significant activation ($p < 0.001$ uncorr.).

even at 100% coherence (Figure 6G), as was the case for first-order stimuli (Figure 6F). Interestingly, the individual IPL responses to second-order and first-order motion, relative to static control, correlated significantly ($r = 0.72$, $p < 0.005$), while there was no significant correlation between individual IPL responses to apparent motion on one hand and first- ($r = 0.31$, $p > 0.2$) or second-order motion ($r = 0.44$, $p > 0.1$) on the other. Comparison of the second-order motion at the three coherence levels to their stationary counterpart revealed a significant IPL activation in the right but not the left hemisphere. This second-order motion site was located more ventrally than the higher-level motion region. The distance between these two activation sites in the right hemisphere was 18 mm in the group analysis and 14 mm averaged over individual subjects (in which a smaller smoothing kernel was used).

Discussion

In this study, we documented a neural correlate of a higher-level salient feature-tracking motion system in

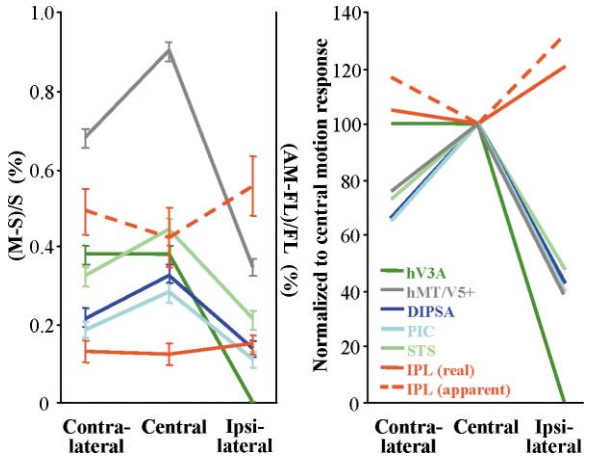

Figure 7. Visual Field Representation in Motion Regions

Motion activation plotted as a function of stimulus position for random texture motion (M-S/S, full lines) and apparent motion (AM-FL/FL, dashed lines) in IPL, early extrastriate regions hMT/V5+, hV3A, and regions in the vicinity of IPL: DIPSA, STS and PIC. (A), absolute values; (B), normalized values to the central motion response. Color list: see inset. In this figure, the ipsilateral values were obtained directly from their local maxima ($p < 0.001$ uncorr. or $p < 0.01$ uncorr., except hV3A), while in Figure 5 they were taken at the local maximum for contralateral motion.

the inferior parietal lobule, using moving isoluminant chromatic gratings. This region contained a bilateral representation of the visual field with a slightly stronger sensitivity in the ipsilateral than central or contralateral field. The same IPL region was selectively activated by another higher order, apparent motion stimulus, but not by second-order motion stimuli. The activation of the IPL region depended on the level of attention to the stimuli in general, but did not reflect a difference in attention to motion and control stimuli. On the other hand, we confirmed that the traditional motion sensitive regions—hV3A, hMT/V5, STS, PIC, POIPS, DIPSM, and DIPSA—correspond to a lower-level luminance-based system. This system processes both first-order and second-order motion stimuli, represents motion predominantly in the contralateral visual field, and magnifies the central part of the visual field.

Several lines of evidence indicate that as one ascends the anatomical hierarchy of the motion processing regions in the monkey, flicker is gradually rejected at further stages (Lagae et al., 1994; Qian and Andersen, 1994). In the present study, flicker responses were also gradually reduced, as reported in earlier imaging studies (Orban et al., 1999; Sunaert et al., 1999; Braddick et al., 2000). Flicker responses were absent in DIPSA, STS, and IPL, suggesting that these regions represent far stages in the human motion-processing hierarchy. At these stages, we demonstrated a functional double dissociation between the lower-level motion areas STS and DIPSA on the one hand and the higher-level IPL motion region on the other. The dissociation was complete in both main experiments 1 and 2. However, when a strong lower order stimulus, in the form of a high-contrast moving random pattern, was used, IPL responded weakly to this stimulus. Thus, our results indicate the existence of two motion-processing systems in the human brain: an energy-driven, contralateral lower-level system, funneling motion information from hMT/V5+ and hV3A into the IPS and STS (Figure 5), and a salience-driven, bilateral higher-level system represented in the inferior parietal lobule (Figures 2 and 6).

Human MT/V5+ responded to all motion stimuli tested. This suggests that it may function as a clearinghouse for motion signals, similar to what has been proposed for striate cortex and luminance signals in general (Zeki, 1978). In monkey, MT/V5 projects to MST (Ungerleider and Desimone, 1986), and this area in turn projects to the retro-insular motion region (Guldin et al., 1992), which is likely to be the homolog of human PIC (Orban et al., 2003). PIC was responsive to higher order motion stimuli and might provide the anatomical link for these signals to reach IPL. The activation of hMT/V5+ in isoluminant conditions is in agreement with recent human imaging studies (Tootell et al., 1995; Wandell et al., 1999) and with single-cell studies in which macaque MT neurons were shown to process chromatically defined motion (Seidemann et al., 1999; Thiele et al., 2001). This activation of hMT/V5+ (and hV3A) is also consistent with the mounting psychophysical evidence of low-level motion energy processing of color input (for review, see Seiffert and Cavanagh, 1999). Finally, the activation of the lower-level motion regions by second-order stimuli is in agreement with the recent studies of Dupont et al. (2003) and Seiffert et al. (2003).

Our results, especially those of main experiment 2, are in excellent agreement with human lesion studies (Battelli et al., 2001; Lê et al., 2002). The representation of higher-level motion in IPL is bilateral. Therefore the effect of unilateral (right) IPL lesions documented by Battelli et al. (2001) might indicate that activity in IPL of both hemispheres is needed to sustain perception of apparent motion. PIC was also responsive to apparent motion at 7 Hz, but given its localization (only 20 mm away from IPL), it may well have been included in the lesion of the Battelli et al. patients. The results of control experiment 5 indicate a possible alternative explanation for Vaina et al.'s dissociation between first- and second-order motion stimuli (Vaina et al., 1999). The lesion in patient DF, although described as dorsal to hMT/V5+ (Vaina et al., 1999), extends posteriorly to the cuneus, possibly compromising the output of hV3A. We observed that hV3A was the only motion region responding well to low-coherence second-order stimuli. Thus, the dissociation reported by Vaina et al. (1999) might indicate that different cortical regions process first-and second-order stimuli at low coherence but not in general.

Our results strongly suggest that lower- and higher order motion regions differ not in the stimuli processed (first or second order) but in the motion processing itself (Cavanagh, 1991), the latter process being feature based, the former energy based. Although these are different processes, they might both compute a change of position over a change in time, the lower-level process over small ranges and the higher-level one over long ranges. The only way for this higher-level process to avoid false matches is by labeling the parts of the image to be matched by saliency. Saliency was explicitly manipulated in the first main experiment, but we suggest that the apparent motion response of IPL is also saliency

based. It has been shown by Gottlieb et al. (1998) that the sudden onset of a stimulus increases its saliency. This view is in agreement with the suggestion made by Lu et al. (1999a) that although salience of a feature can be modulated by attention, the tracking of these features is not dependent on attention. Hence it is not surprising that the IPL region is clearly distinct from the human brain regions involved in directing exogenous and endogenous attention (Corbetta and Shulman, 2002). If lower- and higher order regions compute motion over different spatio-temporal ranges, they complement each other, providing the brain with a more robust mechanism for tracking moving objects over a wider range of conditions, including those of occlusion in cluttered environments. Not surprisingly, Cavanagh (1992) demonstrated psychophysically that tracking of rotating superimposed luminance and color gratings could use either the higher- or lower order motion system. Imaging studies have further revealed that attentive tracking of multiple targets engages the traditional lower-level system along the IPS (Culham et al., 1998, 2001), rather than IPL.

There is increasing evidence of involvement of parietal cortex in motion processing. Following the initial reports (Dupont et al., 1994, 1997; Culham et al., 1998; Sunaert et al., 1999), a series of studies (Orban et al., 1999; Braddick et al., 2000; Jovicich et al., 2001; Beauchamp et al., 2002; Muckli et al., 2002; Schubotz and von Cramon, 2002; Vanduffel et al., 2002; Kriegeskorte et al., 2003) have reported parietal activation by different types of motion stimuli. All these studies used luminance-based stimuli and all activation sites were located in or near the intraparietal sulcus (IPS), not in the inferior parietal lobule (IPL). The closest activation sites in IPS (Jovicich et al., 2001; Schubotz and von Cramon, 2002) were still located 17–19 mm medial, dorsal, and anterior to the higher-level IPL region. IPL, however, has been implicated in the processing of motion in other modalities. Both motion in the auditory and tactile modality activates a number of parietal regions (Griffiths et al., 1998; Lewis et al., 2000; Hagen et al., 2002). Some of these motion regions overlap with lower-level visual motion regions, such as DIPSA (Lewis et al., 2000), but an auditory motion region (66, −26, 26) (Griffiths et al., 1998) and a tactile one (54, −32, 26) (Hagen et al., 2002), both in the IPL, are close to the higher-level visual motion region.

H. Merchant et al. (submitted) have recorded recently in monkey area 7a, a possible homolog of the IPL high-level visual motion region. They documented that a substantial fraction of 7a neurons are indeed responsive to apparent motion over a 2–8 Hz range, as well as to real motion. Furthermore, they showed that many of these neurons are able to code for the location of the moving disc stimuli. This suggests a possible functional underpinning of the complementarity between lower-level and higher-level motion regions. Together they compute the location of a moving target, important in, e.g., interception tasks such as hunting, over a wide range of conditions. The lower order motion regions, however, are likely to perform additional functions on their own. They process motion energy distributions to extract spatial patterns of motion, such as optic flow components (Saito et al., 1986), speed gradients (Duffy and Wurtz, 1997; Xiao et al., 1997), or multicomponent, articulated motion (Perrett et al., 1985). In these operations the explicit information about the position of a moving element is lost. Extraction of spatial motion patterns is important to reconstruct object 3D shape, heading direction, and biological motion, which are critical in visual control of grasping (Vanduffel et al., 2002), of locomotion (Gibson, 1950), and in processing of actions and intentions (Perrett et al., 1985; Frith and Frith, 1999).

While further work is warranted to elucidate the functional role of the different motion regions, the present study clearly establishes the existence of a higher-level motion region in human IPL, with properties distinct from the traditional lower-level motion processing regions.

Experimental Procedures

Six volunteers participated (three male and three female, mean age 21.2 years [19–25]) in the first main experiment, and three of them took part in the first control study (Table 1). In the second control study, 12 subjects participated. Also, 12 subjects participated in the second main experiment (9 male and 3 female, mean age 23.8 years [19–33]), 3 of them were the same as in the former experiments. 2, 6, 7, and 3 of the 12 subjects took part in the third, fourth, fifth and sixth control experiment, respectively. A written informed consent was obtained from all subjects. Subjects fixated a fixation point and eye movements were monitored during all experiments.

In the first main experiment and the first control study, we used isoluminant reddish/greenish sinewave gratings (3° width, 6° height, 3.75 Hz, 0.5 cycle/°) located at 4.5° in the right and left visual field respectively, and viewed monocularly (Figure 1). The gratings were produced by appropriate superposition of sinusoidal modulations of our display device's red, green, and blue primaries. Animation was produced by repetitively presenting a four-frame sequence in which the gratings were phase shifted 90° between successive frames. Low spatial frequency horizontal gratings were used to minimize chromatic aberration and to maximize responses in chromatic visual mechanisms. The stimuli were Gaussian windowed in space and time to avoid the effects of spatio-temporal transients, which favor processing by luminance-based visual mechanisms. The moving and stationary gratings were matched for perceptual strength by measuring contrast detection thresholds using the method of adjustment. Thresholds were measured for each of the eight moving and stationary conditions: low-, medium-, and high-green saturation isoluminant and luminance modulated. These thresholds were obtained from two additional subjects in a separate experiment (same size and eccentricity as in the scanning) and were averaged. The contrasts of the stimuli used during scanning were approximately six times the corresponding detection thresholds. Since detection thresholds were measured for both stationary and moving stimuli, these stimuli were equally salient.

In the second control study, we used a moving and stationary high-contrast random texture pattern (6°/s, eight random directions, as in Sunaert et al. [1999]) positioned centrally (3° diameter), or in the right or left visual field (5° diameter) at 5° eccentricity, and viewed binocularly.

The stimulus in the second main experiment (Figure 6A) consisted of two alternating frames, each with two diagonally opposed white dots (0.5° diameter) arrayed on the two opposite vertices of a 2° square or diamond, at a temporal frequency of 2 and 7 Hz. If the interval between the successive frames is appropriate, apparent motion of two dots in either horizontal or vertical direction is perceived. The stimulus was positioned at 4° eccentricity in the left and right visual field and was viewed binocularly. The control condition consisted of four dots presented simultaneously (7 Hz).

In a third control experiment, the apparent motion stimulus (7 Hz) and the simultaneously presented dots (7 Hz) were positioned centrally or 4° in left or right visual field. In this and subsequent control experiments, stimuli were viewed binocularly.

In control experiment 4 the apparent motion stimulus (7 Hz) and the simultaneously presented dots (7 Hz) were presented 4° in right

and left visual field. The subjects' task was to signal with a key press (R index finger, response window 1000 ms) the increase in temporal frequency of these stimuli (to 12 Hz for apparent motion and to 15 Hz for flicker). The increase (lasting 800 ms) occurred on average twice per scanning epoch (range: one to five times). Subjects underwent a 2 hr training session before the scanning. Average performance in the four task conditions ranged between 94% and 97% correct (NS, ANOVA $p > 0.15$). Reaction times were also very similar (NS, ANOVA, $p > 0.1$) ranging between 668 and 698 ms.

The stimuli in control experiments 5 and 6 were contrast-modulated checkerboards ($10^\circ \times 10^\circ$), as described by Vaina and Cowey (1996), presented centrally. The stimuli consisted of moving (4°/s, eight random directions) or stationary $0.2^\circ \times 0.2^\circ$ square texture micropatterns on a background of flickering random texture. The contrast of the micropatterns (60%) differed from that of the flickering background texture (20%), but the mean luminance was identical. Before each scanning session, the LCD projector was calibrated and γ corrected. In experiment 5, the strength of the motion signal was varied by changing the proportion of coherently moving micropatterns (30%, 65%, and 100%) at a constant density of 1.6. In control experiment 6, the density was varied (0.32%, 1.6%, and 8%) at a constant coherence of 100%.

Visual stimuli were projected from a Barco 6300 LCD projector (1280×1024; 60 Hz refresh rate) onto a screen 36 cm (experiment 1 and first control) or 28 cm (other experiments) in front of the subjects' eyes. In the first main experiment and first control study, a magenta theater gel (Lee Pink 002) placed over the projection lens reduced the disproportionately high luminance of the green primary to levels appropriate for our experiments. The projection system was carefully calibrated for γ correction and for the final chromaticities of the red (0.639, 0.301), green (0.294, 0.314), and blue (0.143, 0.031) primaries using a Minolta CS-100 Chroma Meter (Mayer International Ltd., UK). The reddish and greenish components of our gratings were rendered isoluminant using a motion nulling technique, as described by Lu et al. (1999a, 1999b). Briefly, we employed four frame animation sequences for each reddish/greenish grating as in the main experiment, except that the odd numbered frames consisted of 10% achromatic luminance gratings instead of a reddish/greenish grating. The reddish component of the chromatic gratings was held constant in radiance amplitude, and the radiance amplitude of the antiphase greenish component was varied. In this configuration, there was an unambiguous signal for luminance motion in one direction when the red bars were more luminous than the green, an unambiguous motion signal in the opposite direction when green was more luminous than red, and directionally ambiguous motion when red and green were isoluminant for a particular observer (the actual "red" direction varied randomly from trial to trial). We used the method of constant stimuli to determine the isoluminance points at each salience level employed in the first main and control experiment. Psychometric functions were fit to the data and analyzed using routines published by Foster and Bischof (1991). The 95% confidence intervals around the estimated isoluminance points were typically 4%–8%. Isoluminance points were obtained in the scanner before the start of each of the six (two) scanning sessions that each subject underwent in experiment 1 (control study 1). We believe this methodology eliminated the possibility that our results could be attributed to unwanted luminance artifacts in our presumptively "isoluminant" stimuli.

The experiments used block designs with the presentation order of the conditions randomized within and between different time series and subjects. Except in main experiment 2, each time series included fixation-only conditions as a baseline reference. A scanning session included seven to ten time series depending on the duration of the time series. Each functional volume consisted of gradient-echo echoplanar whole-brain images (Siemens, 1.5T Sonata; TR = 3010 ms, TE = 50 ms, flip angle 90°, 64×64 matrix, $3 \times 3 \times 4.5$ mm voxels, 32 sagittal slices). In total, we collected 6992 functional volumes over six sessions per subject ($n = 6$) in main experiment 1, 2432 over 2 sessions per subject in the first control study ($n = 3$), 1260 in 1 session per subject in the second control study ($n = 12$), 1200 in 1 session per subject in main experiment 2 ($n = 12$), 1650 ($n = 2$), 1400 ($n = 6$), 1350 ($n = 7$), and 1400 ($n = 3$) in one session per subject in the third, fourth, fifth, and sixth control experiment respectively. Subjects were immobilized using an individually molded bite-bar. Fixation was controlled using a MR compatible eye movement tracking device (Ober2; Permobil Meditech, Timra, Sweden). A high-resolution anatomical image (3D-MPRAGE) was acquired for each subject (TR = 1950 ms, TE = 3.9 ms, TI = 800 ms, 240×256 matrix, $1 \times 1 \times 1$ mm voxels, 160 sagittal partitions).

Data were analyzed using Statistical Parametric Mapping version SPM99 (Wellcome Department of Cognitive Neurology, London, UK). The functional volumes were coregistered with the anatomical image, realigned and stereotactically normalized into the Montreal Neurologic Institute template in Talairach space (Talairach and Tournoux, 1988). The data were spatially smoothed with an isotropic Gaussian kernel (group analyses: 6 mm; single-subject analyses: 4 mm). For each stimulus comparison, significant MR signal changes were assessed using a map of z scores. For fixed-effect group analyses the threshold was set at $p < 0.05$ corrected for multiple comparisons. In single-subject analyses and in the presence of a priori information in group analyses, a threshold of $p < 0.001$ uncorrected for multiple comparisons was used. For the stringent random-effect analysis, $p < 0.0001$ uncorrected was used as threshold.

Acknowledgments

We thank Y. Celis, M. De Paep, W. Depuydt, P. Kayenbergh, and G. Meulemans for technical support. We are grateful to Dr. R. Vogels, Dr. W. Vanduffel, and Dr. J. Todd for invaluable comments on the manuscript and Prof. P. Van Hecke for access to the scanner. Supported by grants GOA 2000/11, IUAP 5/04, FWO G.0401.00, and from the UIA. (K.G.C.).

Received: April 9, 2003
Revised: July 10, 2003
Accepted: September 3, 2003
Published: October 29, 2003

References

Battelli, L., Cavanagh, P., Intriligator, J., Tramo, M.J., Hénaff, M.-A., Michèl, F., and Barton, J.J.S. (2001). Unilateral right parietal damage leads to bilateral deficit for high-level motion. Neuron *32*, 985–995.

Beauchamp, M.S., Lee, K.E., Haxby, J.V., and Martin, A. (2002). Parallel visual motion processing streams for manipulable objects and human movements. Neuron *34*, 149–159.

Braddick, O. (1974). A short-range process in apparent motion. Vision Res. *14*, 519–527.

Braddick, O.J., O'Brien, J.M., Wattam-Bell, J., Atkinson, J., and Turner, R. (2000). Form and motion coherence activate independent, but not dorsal/ventral segregated, networks in the human brain. Curr. Biol. *10*, 731–734.

Cavanagh, P. (1991). Short-range vs long-range motion: not a valid distinction. Spat. Vis. *5*, 303–309.

Cavanagh, P. (1992). Attention-based motion perception. Science *257*, 1563–1565.

Cavanagh, P., and Mather, G. (1989). Motion: the long and short of it. Spat. Vis. *4*, 103–129.

Chubb, C., and Sperling, G. (1988). Drift-balanced random stimuli: a general basis for studying non-Fourier motion perception. J. Opt. Soc. Am. A *5*, 1986–2007.

Corbetta, M., and Shulman, G.L. (2002). Control of goal-directed and stimulus-driven attention in the brain. Nat. Rev. Neurosci. *3*, 201–215.

Culham, J.C., Brandt, S.A., Cavanagh, P., Kanwisher, N.G., Dale, A.M., and Tootell, R.B.H. (1998). Cortical fMRI activation produced by attentive tracking of moving targets. J. Neurophysiol. *80*, 2657–2670.

Culham, J.C., Cavanagh, P., and Kanwisher, N.G. (2001). Attention response functions: characterizing brain areas using fMRI activation during parametric variations of attentional load. Neuron *32*, 737–745.

Duffy, C.J., and Wurtz, R.H. (1997). Medial superior temporal area neurons respond to speed patterns in optic flow. J. Neurosci. *17*, 2839–2851.

Dupont, P., Orban, G.A., De Bruyn, B., Verbruggen, A., and Mortel-

mans, L. (1994). Many areas in the human brain respond to visual motion. J. Neurophysiol. *72*, 1420–1424.

Dupont, P., De Bruyn, B., Vandenberghe, R., Rosier, A.M., Michiels, J., Marchal, G., Mortelmans, L., and Orban, G.A. (1997). The kinetic occipital region in human visual cortex. Cereb. Cortex *7*, 283–292.

Dupont, P., Sary, G., Peuskens, H., and Orban, G.A. (2003). Cerebral regions processing first- and higher-order motion in an opposed-direction discrimination task. Eur. J. Neurosci. *17*, 1509–1517.

Exner, S. (1875). Experimentelle untersuchung der einfachsten psychishen. Processe. Archiv für die Gesamte Physiologie des Menschen und der Tiere *11*, 403–432.

Foster, D.H., and Bischof, W.F. (1991). Thresholds from psychometric functions: superiority of bootstrap to incremental and probit variance estimators. Psychol. Bull. *109*, 152–159.

Friston, K.J., Holmes, A.P., Price, C.J., Büchel, C., and Worsley, K.J. (1999). Multisubject fMRI studies and conjunction analyses. Neuroimage *10*, 385–396.

Frith, C.D., and Frith, U. (1999). Interacting minds-a biological basis. Science *286*, 1692–1695.

Gibson, J.J. (1950). The Perception of the Visual World (Boston: Houghton-Mifflin).

Goebel, R., Khorram-Sefat, D., Muckli, L., Hacker, H., and Singer, W. (1998). The constructive nature of vision: direct evidence from functional magnetic resonance imaging studies of apparent motion and motion imagery. Eur. J. Neurosci. *10*, 1563–1573.

Gottlieb, J.P., Kusunoki, M., and Goldberg, M.E. (1998). The representation of visual salience in monkey parietal cortex. Nature *391*, 481–484.

Griffiths, T.D., Rees, G., Rees, A., Green, G.G.R., Witton, C., Rowe, D., Buchel, C., Turner, R., and Frackowiak, R.S.J. (1998). Right parietal cortex is involved in the perception of sound movement in humans. Nat. Neurosci. *1*, 74–79.

Guldin, W.O., Akbarian, S., and Grusser, O.J. (1992). Cortico-cortical connections and cytoarchitectonics of the primate vestibular cortex: a study in squirrel monkeys. J. Comp. Neurol. *326*, 375–401.

Hagen, M.C., Franzén, O., McGlone, F., Essick, G., Dancer, C., and Pardo, J.V. (2002). Tactile motion activates the human middle temporal/V5 (MT/V5) complex. Eur. J. Neurosci. *16*, 957–964.

Jovicich, J., Peters, R.J., Koch, C., Braun, J., Chang, L., and Ernst, T. (2001). Brain areas specific for attentional load in a motion-tracking task. J. Cogn. Neurosci. *13*, 1048–1058.

Kriegeskorte, N., Sorger, B., Naumer, M., Schwarzbach, J., van den Boogert, E., Hussy, W., and Goebel, R. (2003). Human cortical object recognition from a visual motion flowfield. J. Neurosci. *23*, 1451–1463.

Lagae, L., Maes, H., Raiguel, S., Xiao, D.K., and Orban, G.A. (1994). Responses of macaque STS neurons to optic flow components: a comparison of areas MT and MST. J. Neurophysiol. *71*, 1597–1626.

Lê, S., Cardebat, D., Boulanouar, K., Hénaff, M.-A., Michel, F., Milner, D., Dijkerman, C., Puel, M., and Démonet, J.-F. (2002). Seeing, since childhood, without ventral stream: a behavioural study. Brain *125*, 58–74.

Lewis, J.W., Beauchamp, M.S., and DeYoe, E.A. (2000). A comparison of visual and auditory motion processing in human cerebral cortex. Cereb. Cortex *10*, 873–888.

Lu, Z.-L., and Sperling, G. (1995). Attention-generated apparent motion. Nature *377*, 237–239.

Lu, Z.-L., Lesmes, L.A., and Sperling, G. (1999a). The mechanism of isoluminant chromatic motion perception. Proc. Natl. Acad. Sci. USA *96*, 8289–8294.

Lu, Z.-L., Lesmes, L.A., and Sperling, G. (1999b). Perceptual motion standstill in rapidly moving chromatic displays. Proc. Natl. Acad. Sci. USA *96*, 15374–15379.

Muckli, L., Singer, W., Zanella, F.E., and Goebel, R. (2002). Integration of multiple motion vectors over space: an fMRI study of transparent motion perception. Neuroimage *16*, 843–856.

Orban, G.A., Sunaert, S., Todd, J.T., Van Hecke, P., and Marchal, G. (1999). Human cortical regions involved in extracting depth from motion. Neuron *24*, 929–940.

Orban, G.A., Fize, D., Peuskens, H., Denys, K., Nelissen, K., Sunaert, S., Todd, J., and Vanduffel, W. (2003). Similarities and differences in motion processing between the human and macaque brain: evidence from fMRI. Neuropsychologia, in press.

Perrett, D.I., Smith, P.A., Mistlin, A.J., Chitty, A.J., Head, A.S., Potter, D.D., Broennimann, R., Milner, A.D., and Jeeves, M.A. (1985). Visual analysis of body movements by neurones in the temporal cortex of the macaque monkey: a preliminary report. Behav. Brain Res. *16*, 153–170.

Puce, A., Allison, T., Bentin, S., Gore, J.C., and McCarthy, G. (1998). Temporal cortex activation in humans viewing eye and mouth movements. J. Neurosci. *18*, 2188–2199.

Qian, N., and Andersen, R.A. (1994). Transparent motion perception as detection of unbalanced motion signals. II. Physiology. J. Neurosci. *14*, 7367–7380.

Rees, G., Frith, C.D., and Lavie, N. (1997). Modulating irrelevant motion perception by varying attentional load in an unrelated task. Science *278*, 1616–1619.

Rees, G., Friston, K., and Koch, C. (2000). A direct quantitative relationship between the functional properties of human and macaque V5. Nat. Neurosci. *3*, 716–723.

Saito, H., Yukie, M., Tanaka, K., Hikosaka, K., Fukada, Y., and Iwai, E. (1986). Integration of direction signals of image motion in the superior temporal sulcus of the macaque monkey. J. Neurosci. *6*, 145–157.

Schubotz, R.I., and von Cramon, D.Y. (2002). A blueprint for target motion: fMRI reveals perceived sequential complexity to modulate premotor cortex. Neuroimage *16*, 920–935.

Seidemann, E., Poirson, A.B., Wandell, B.A., and Newsome, W.T. (1999). Color signals in area MT of the macaque monkey. Neuron *24*, 911–917.

Seiffert, A.E., and Cavanagh, P. (1999). Position-based motion perception for color and texture stimuli: effects of contrast and speed. Vision Res. *39*, 4172–4185.

Seiffert, A.E., Somers, D.C., Dale, A.M., and Tootell, R.B.H. (2003). Functional MRI studies of human visual motion perception: texture, luminance, attention and after-effects. Cereb. Cortex *13*, 340–349.

Smith, A.T., Greenlee, M.W., Singh, K.D., Kraemer, F.M., and Hennig, J. (1998). The processing of first- and second-order motion in human visual cortex assessed by functional magnetic resonance imaging (fMRI). J. Neurosci. *18*, 3816–3830.

Sunaert, S., Van Hecke, P., Marchal, G., and Orban, G.A. (1999). Motion-responsive regions of the human brain. Exp. Brain Res. *127*, 355–370.

Talairach, J., and Tournoux, P. (1988). Co-Planar Stereotaxic Atlas of the Human Brain (New York: Thieme).

Ternus, J. (1938). The problem of phenomenal identity. In A Source Book of Gestalt Psychology, W.D. Ellis, ed. (London: Rotledge and Kegan Paul), pp. 149–160.

Thiele, A., Dobkins, K.R., and Albright, T.D. (2001). Neural correlates of chromatic motion perception. Neuron *32*, 351–358.

Tootell, R.B.H., Reppas, J.B., Kwong, K.K., Malach, R., Born, R.T., Brady, T.J., Rosen, B.R., and Belliveau, J.W. (1995). Functional analysis of human MT and related visual cortical areas using magnetic resonance imaging. J. Neurosci. *15*, 3215–3230.

Tootell, R.B.H., Mendola, J.D., Hadjikhani, N.K., Ledden, P.J., Liu, A.K., Reppas, J.B., Sereno, M.I., and Dale, A.M. (1997). Functional analysis of V3A and related areas in human visual cortex. J. Neurosci. *17*, 7060–7078.

Ungerleider, L.G., and Desimone, R. (1986). Cortical connections of visual area MT in the macaque. J. Comp. Neurol. *248*, 190–222.

Vaina, L.M., and Cowey, A. (1996). Impairment of the perception of second order motion but not first order motion in a patient with unilateral focal brain damage. Proc. R. Soc. Lond. B. Biol. Sci. *263*, 1225–1232.

Vaina, L.M., Cowey, A., and Kennedy, D. (1999). Perception of first-

and second-order motion: separable neurological mechanisms? Hum. Brain Mapp. *7*, 67–77.

Vanduffel, W., Fize, D., Peuskens, H., Denys, K., Sunaert, S., Todd, J.T., and Orban, G.A. (2002). Extracting 3D from motion: differences in human and monkey intraparietal cortex. Science *298*, 413–415.

Wandell, B.A., Poirson, A.B., Newsome, W.T., Baseler, H.A., Boynton, G.M., Huk, A., Gandhi, S., and Sharpe, L.T. (1999). Color signals in human motion-selective cortex. Neuron *24*, 901–909.

Wertheimer, M. (1912). Experimentelle studien über das sehen von bewegung. Z. Psychol. *61*, 161–265.

Xiao, D.K., Marcar, V.L., Raiguel, S.E., and Orban, G.A. (1997). Selectivity of macaque MT/V5 neurons for surface orientation in depth specified by motion. Eur. J. Neurosci. *9*, 956–964.

Zeki, S.M. (1978). Functional specialisation in the visual cortex of the rhesus monkey. Nature *274*, 423–428.

Zeki, S., Watson, J.D., Lueck, C.J., Friston, K.J., Kennard, C., and Frackowiak, R.S. (1991). A direct demonstration of functional specialization in human visual cortex. J. Neurosci. *11*, 641–649.

Zhuo, Y., Zhou, T.G., Rao, H.Y., Wang, J.J., Meng, M., Chen, M., Zhou, C., and Chen, L. (2003). Contributions of the visual ventral pathway to long-range apparent motion. Science *299*, 417–420.